A Spatially filtered data from simulation $\mathcal{S}_\bullet$ and $\mathcal{S}_\circ$

Results from simulation $\mathcal{S}_\bullet$ and $\mathcal{S}_\circ$, after applying a circular low-pass filter with a diameter of 4500 m are given here.

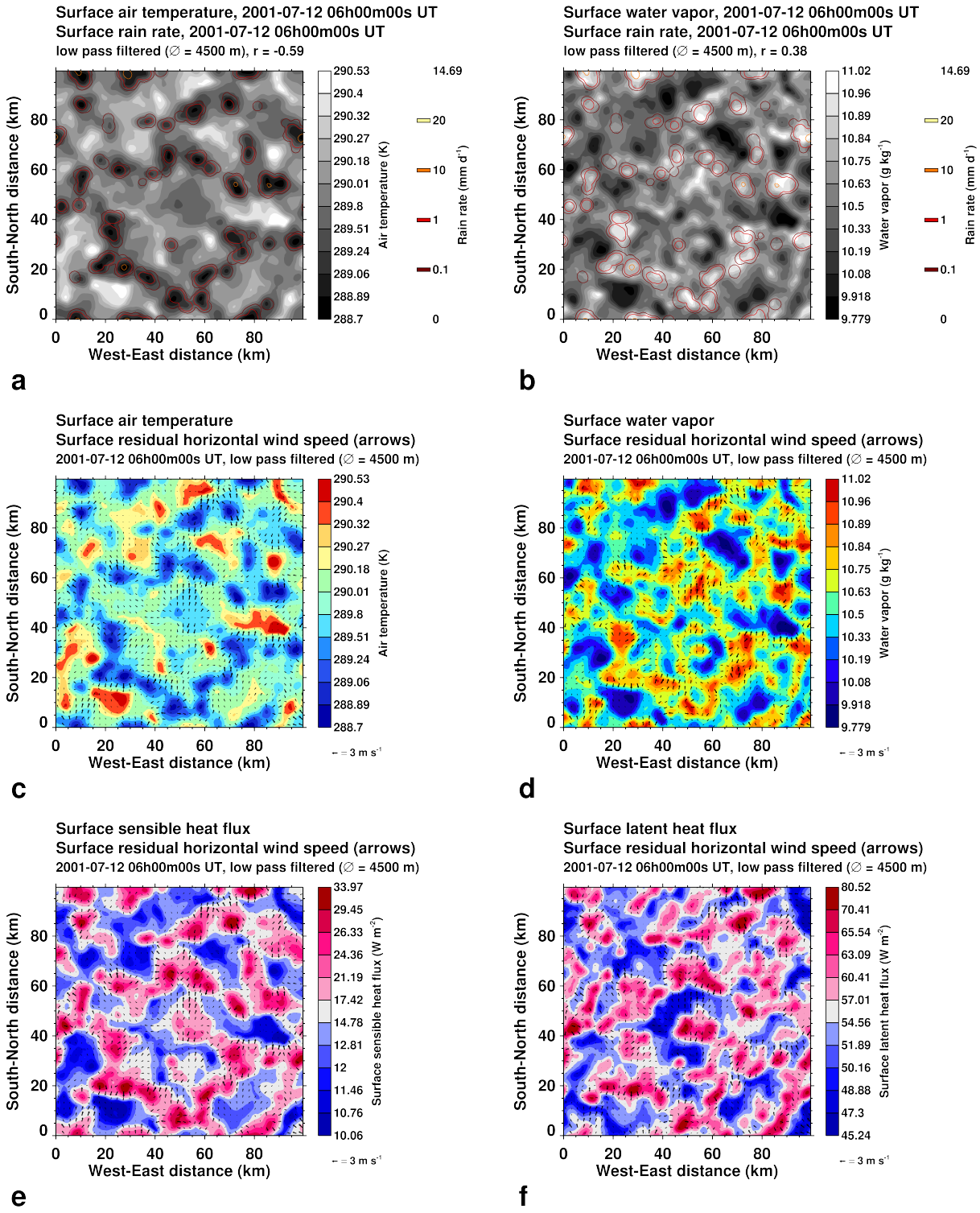

Fig. A-1. Surface rain rate with surface air temperature (a) and surface water vapor (b); surface air temperature (c) and water vapor (d) with the residual horizontal surface wind field; and the surface sensible (e) and latent (f) heat flux with the residual horizontal surface wind field, in simulation $\mathcal{S}_\circ$, after applying a circular low-pass filter with a diameter of 4500 m. The color scales are bounded by the minimum and maximum of the data. Minimum and maximum line contours are suppressed.

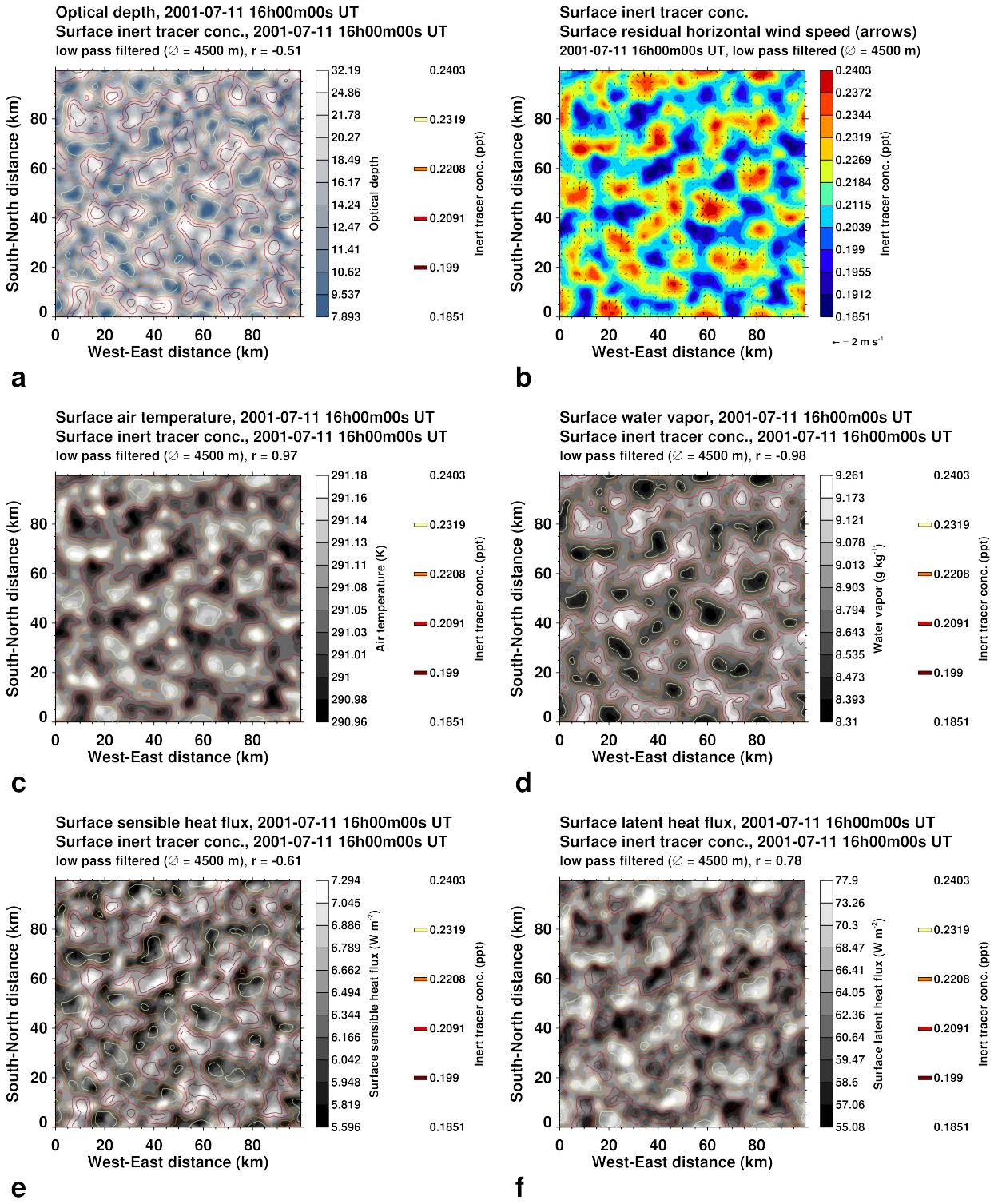

Fig. A-2. Surface concentration of the inert tracer, with (a) cloud optical depth, (b) residual horizontal surface wind field, (c) surface air temperature, (d) surface water vapor, and surface sensible (e) and latent (f) heat flux, in simulation $\mathcal{S}_\bullet$, after applying a circular low-pass filter with a diameter of 4500 m. The color scales are bounded by the minimum and maximum of the data. Minimum and maximum line contours are suppressed.

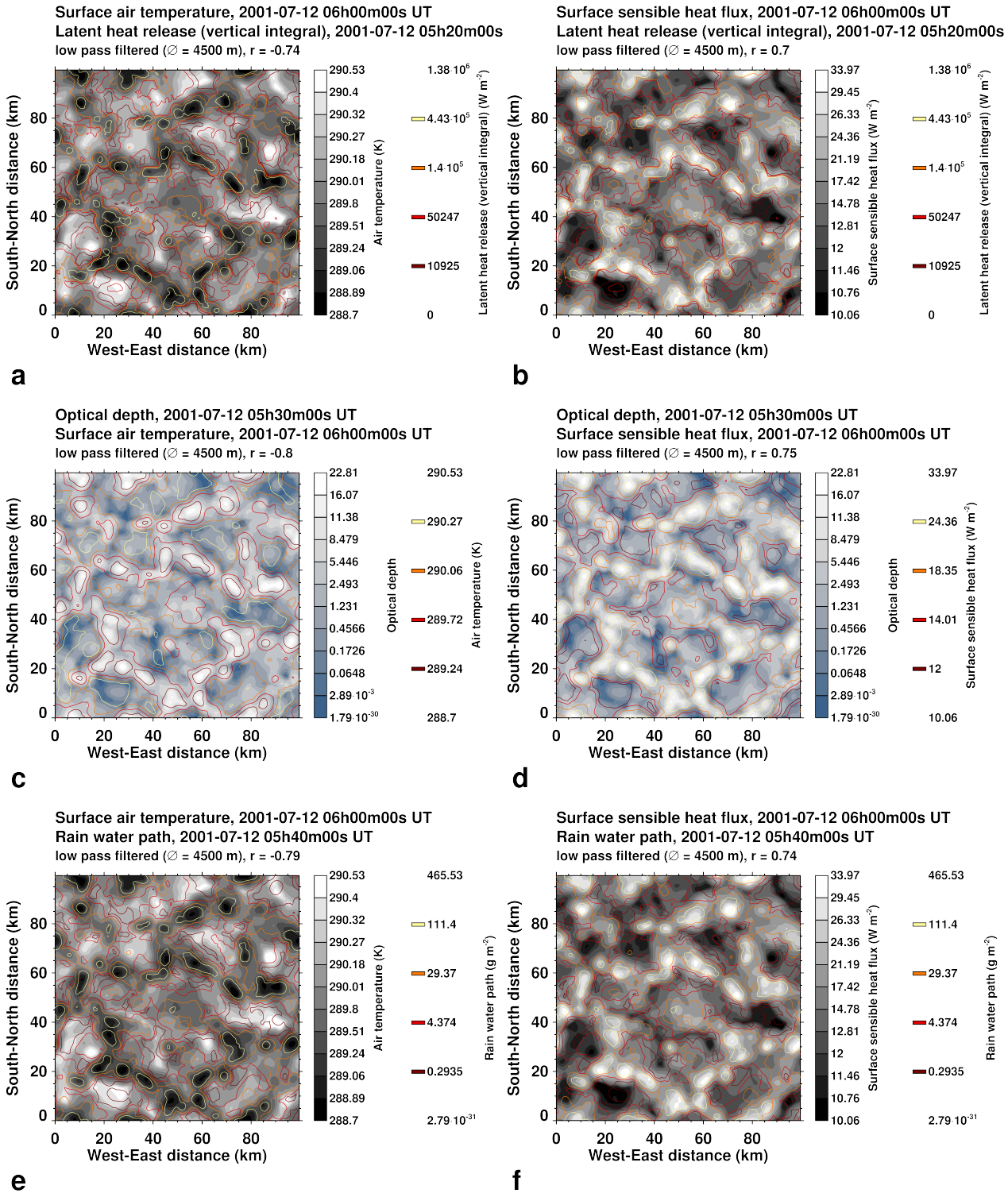

Fig. A-3. Lagged correlation of the latent heat release path with (a) surface air temperature and (b) surface sensible heat flux, of cloud optical depth with (c) surface air temperature and (d) surface sensible heat flux, and of the rain water path with (e) surface air temperature and (f) surface sensible heat flux, in simulation $\mathcal{S}_\circ$, after applying a circular low-pass filter with a diameter of 4500 m. The color scales are bounded by the minimum and maximum of the data. Minimum and maximum line contours are suppressed.

B Simulation $\mathcal{S}'_\circ$

Results from simulation $\mathcal{S}'_\circ$ are given here and compared with results from simulation $\mathcal{S}_\circ$.

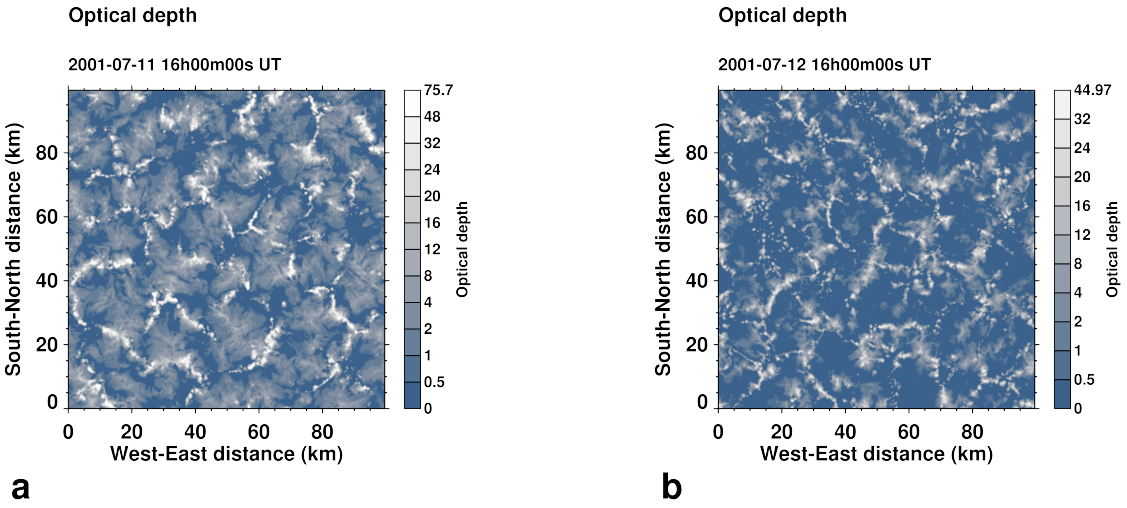

Fig. B-1. Cloud optical depth in simulation $\mathcal{S}'_\circ$ after 12 (a) and 24h (b). The color scale extends to the cloud optical depth maximum.

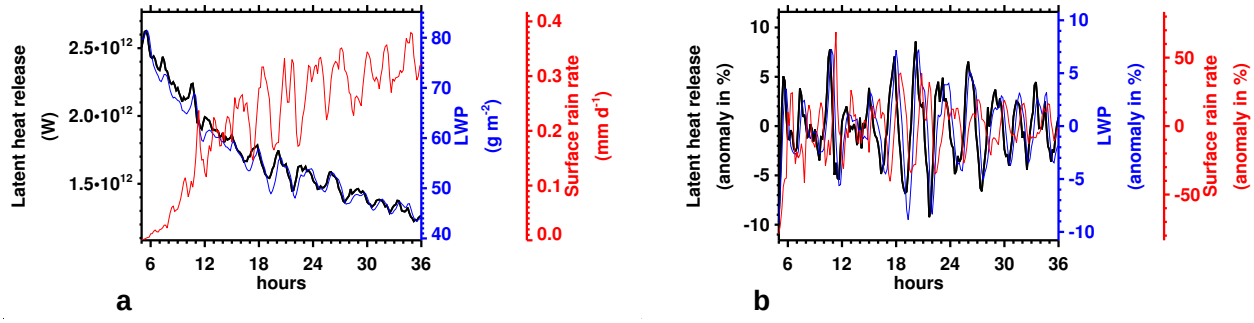

Fig. B-2. (a) domain-integrated latent heat release (heating of the air from condensation of water vapor), domain-averaged liquid water path and surface rain, and (b) their temporal anomalies (against a 3 h running mean) in simulation $\mathcal{S}'_{\circ}$.

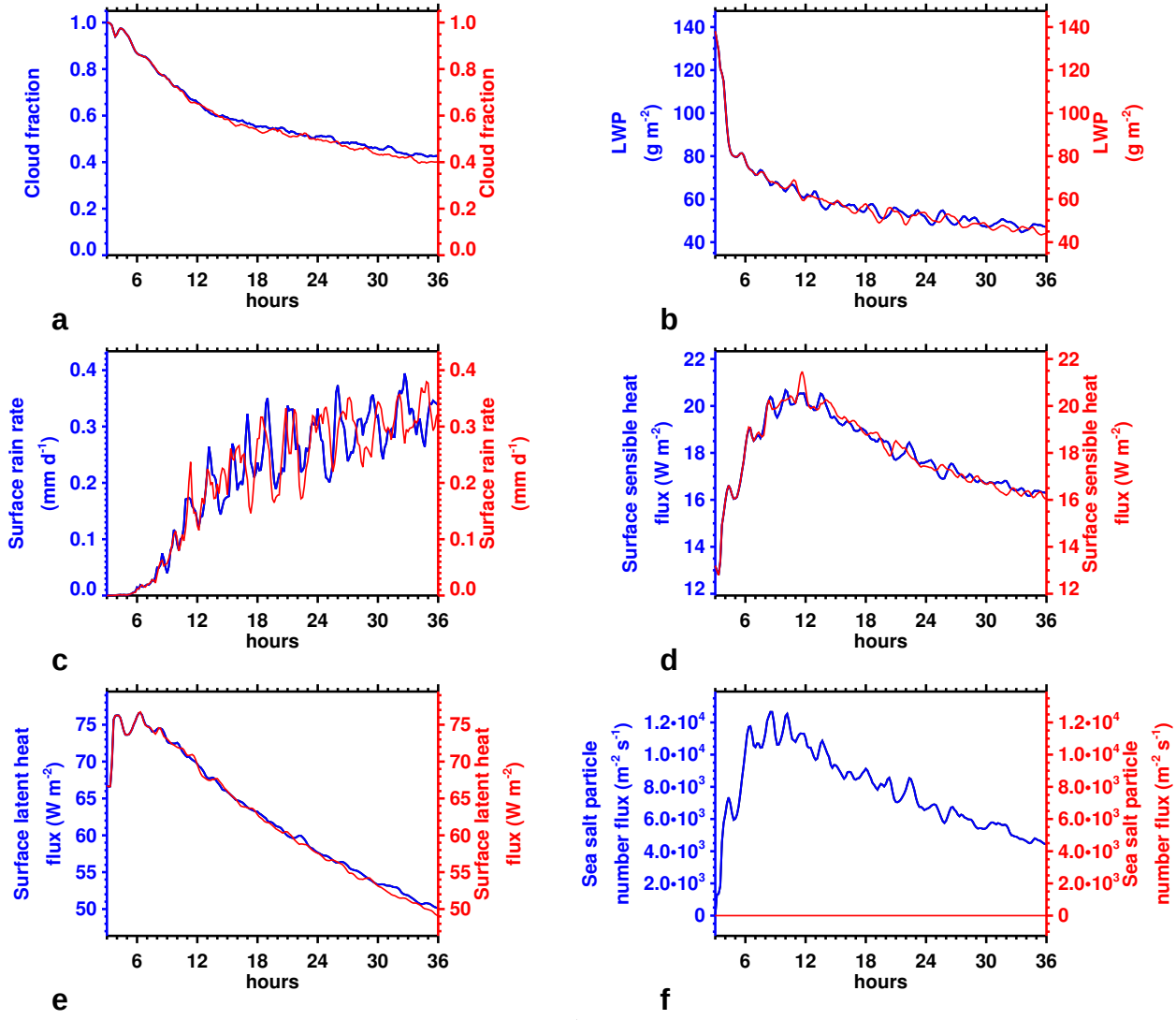

Fig. B-3. Domain-averaged time series of selected quantities in simulation $\mathcal{S}_\circ$ (blue) and $\mathcal{S}'_\circ$ (red).

C Simulation $\mathcal{S}_{\circ}''$

Results from simulation $\mathcal{S}_{\circ}''$ are given here and compared with results from simulation $\mathcal{S}_{\circ}$.

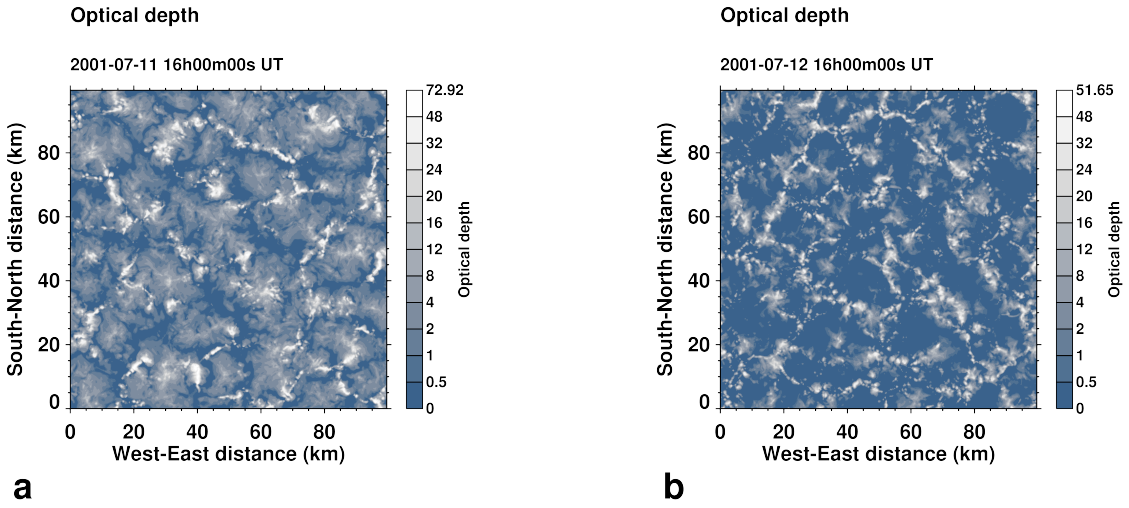

Fig. C-1. Cloud optical depth in simulation $\mathcal{S}_{\circ}''$ after 12 (a) and 24h (b). The color scale extends to the cloud optical depth maximum.

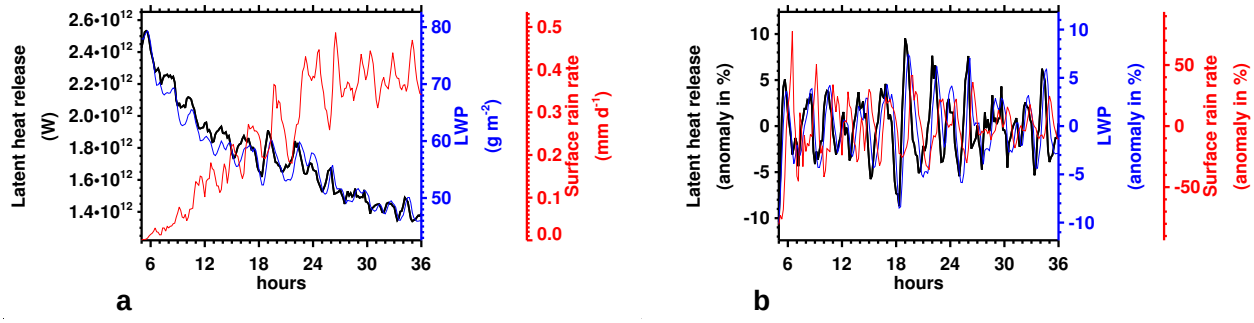

Fig. C-2. (a) domain-integrated latent heat release (heating of the air from condensation of water vapor), domain-averaged liquid water path and surface rain, and (b) their temporal anomalies (against a 3 h running mean) in simulation $\mathcal{S}''_{\circ}$.

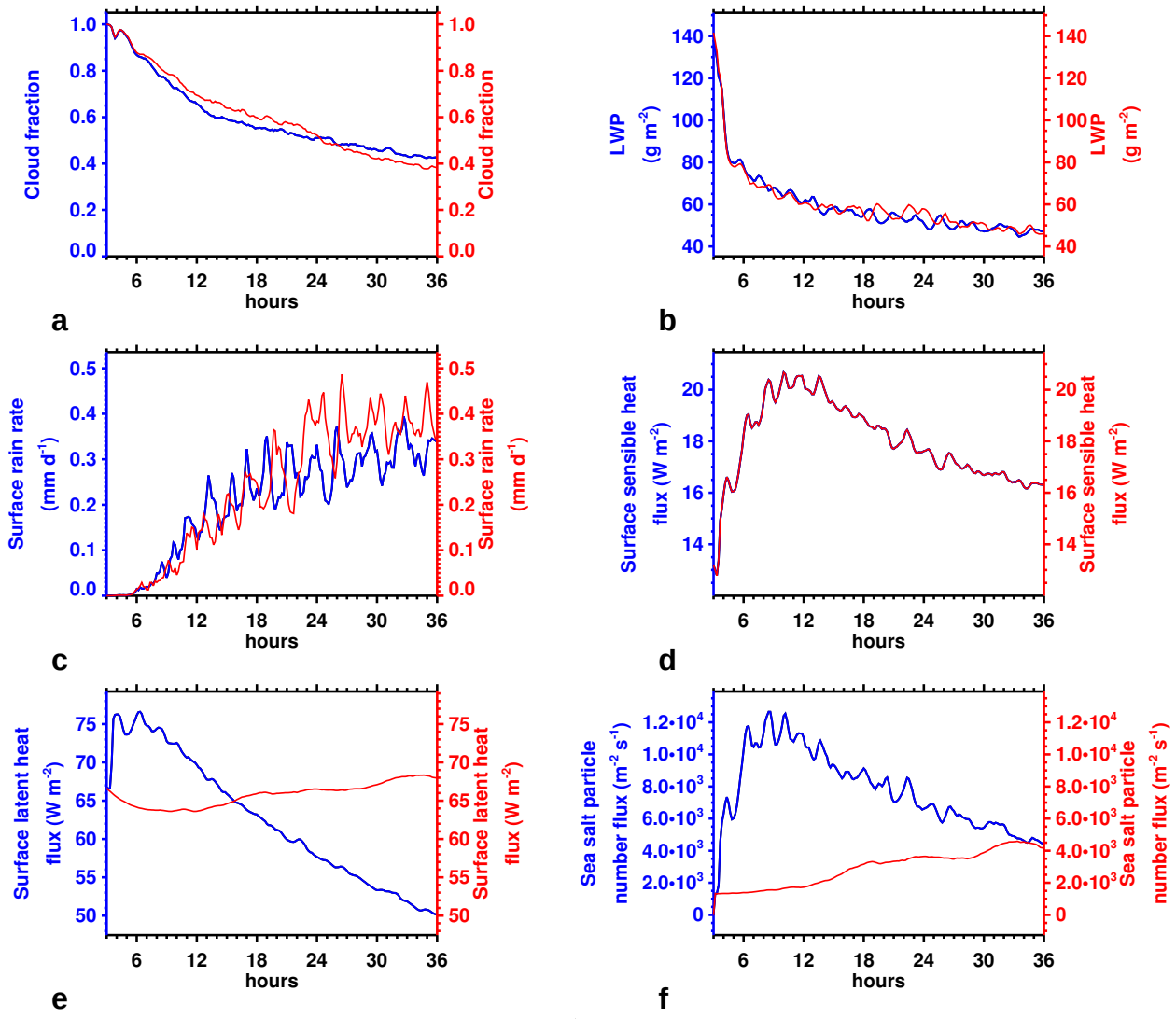

Fig. C-3. Domain-averaged time series of selected quantities in simulation $\mathcal{S}_\circ$ (blue) and $\mathcal{S}''_\circ$ (red).